

Short Communication

Effects of Graphene Addition on Negative Active Material and Lead Acid Battery performances under Partial State of Charge Condition

Witanty¹, Oxi Putra Merdeka¹, Lia Amalia¹, Lukman Noerochim², Heru Setyawan³,
Abdullah Shahab¹, Suwarno Suwarno^{1,*}

¹ Department of Mechanical Engineering, ITS, Surabaya 60111, Indonesia

² Department of Material and Metallurgical Engineering, ITS, Surabaya 60111, Indonesia

³ Department of Chemical Engineering, ITS, Surabaya 60111, Indonesia

*E-mail: warno@me.its.ac.id

Received: 1 March 2021 / *Accepted:* 10 June 2021 / *Published:* 30 June 2021

The use of carbon materials as additives in lead-acid battery electrodes is known to have a positive effect on battery performance via the increase in the battery cycle life. However, every type of carbon material has a different impact. Furthermore, the mechanism of performance improvement must be clarified. In the present work, graphene was added into a negative active material (NAM) used in a battery cell. The cell was tested under a partial state of charge condition at an extreme discharge cycle. The NAM plates were also tested using cyclic voltammetry and electrochemical impedance spectroscopy. The results showed that the graphene additive increases the conductance of the NAM. Scanning electron images showed refined particle sizes of the sulfates. A combination of decreasing the internal resistance of the battery and particle refinement of the NAM was found to be responsible for the improved cycle life.

Keywords: Graphene, Lead-acid battery, Life cycle, PSOC test

1. INTRODUCTION

Since the invention of Lead-acid batteries (LABs) about 160 years ago, they have evolved considerably over the years. LABs remain among the most widely used secondary batteries because of their price. It is well-known that a LAB has relatively low values of specific capacity and specific energy along with low utilization efficiency of the active mass in conjunction with the heavyweight of a conventional grid. However, these shortcomings are not relevant when LABs are used as stationary batteries for renewable energy applications, thus allowing for their use in the future [1].

The problem that arises when using a LAB as a stationary battery is the non-conductive PbSO_4 formed at both negative and positive electrodes at the discharge state that is known to hinder the dissolution of the sulfation upon charging [2]. The depth of discharge or partial charging of the battery results in a significantly shortened battery life. Batteries for renewable energy system application sometimes must overcome the high depth of discharge (DoD) and in a partial state of charge (PSOC) condition, resulting in fast electrode degradation via sulfation of the negative plate in a lead-acid battery [3]. LABs for energy storage applications are often operated at high DoD and PSOC conditions [4,5].

Some research [5,6] showed that sulfation (PbSO_4) in negative electrodes is more severe than that in positive electrodes. Other work [6] showed that sulfation rapidly increases the battery's internal resistance and reduces the water in electrolyte. Researchers [7,8] suggested using carbon as an additive in a negative active material (NAM) to overcome the problem. The use of carbon is said to achieve the following: 1) flatten the attachment of lead sulfate molecules to the cross-sections of the NAM, 2) reduce the discharge and charge current densities, and 3) provide a network of conductors during charging to facilitate the decomposition of lead sulfate [9,10]. The carbon material in the H_2SO_4 solution also functions as a capacitor with two layers of electrodes initially storing the charge when charging and discharging, thereby providing additional time for the electrochemical process [11,12]. Fernandez, Pavlov, and others highlighted the benefits of using additive carbon in the NAM to extend the cycle performance [13–16].

Graphene material is known to have a very high conductivity and a very high surface area; therefore, it is a promising material for use as an additive in LAB active materials [17]. Previous research also showed that the addition of graphene oxide increased the battery life cycle to a greater degree than other additives of carbon-based materials [18]. However, the dimensionality and surface properties of graphene apparently affected the LAB performances [18–20]. Thus, a study focused on how the use of graphene affects the LAB properties is required. In the present work, the effect of graphene addition on the battery's cycle life under PSOC conditions at a lower half DoD was studied to investigate the mechanism of improved cycle life of a LAB with the addition of graphene.

2. RESEARCH METHOD

2.1. Preparation of negative plate and battery cell

The negative active material (NAM) was prepared with and without the addition of graphene. The NAM without graphene was prepared using 90 wt. % lead oxide (PbO) powder from SAP Chemical, H_2SO_4 with 1.26 sp. gr. concentration, and pure H_2O as the solvent. 100 gr of lead oxide powder was milled using a ceramic pounder until it was fine enough. Next, the milled lead oxide was poured into a beaker glass equipped with a thermometer. The powder was then stirred for two minutes. While stirring, 5.86 ml of H_2O was added and mixed with the powder. At this stage, the mixture looked like yellowish mud. The stirring continued for 30 minutes. Afterwards, 14.14 ml of H_2SO_4 was added to the mixture gradually using a pipette and then was closely monitored for the temperature change to ensure that the mixture remained below 50°C . The stirring was performed manually using a

glass spatula. After stirring, semi-solid particles were found in the mixture, which was pinkish in color and had the consistency of cement.

The NAM with the addition of 0.2 wt.% graphene was prepared similar to the NAM without graphene, except 0.2 g graphene was added in the first stage of the process. The synthesis and properties of graphene were similar to those described in a previous publication [21]. When the mixture preparation was completed, it contained semi-solid particles, black in color, and had the consistency of cement.

Next, the pasting process was performed. A commercial grid was cut into a rectangular shape of $0.75\text{cm} \times 1\text{ cm}$ in size for each specimen. Each grid specimen was placed above a glass mat. Next, the NAM was smeared onto each specimen to cover all of the surfaces of the grid manually using a stainless steel scrapper. After the pasting process, the grid underwent the curing process.

The curing process was performed for 24 hours using a furnace equipped with temperature and moisture sensors. A tray filled with water was placed below a rack inside the furnace to allow the water to vaporize and moisturize the furnace. The plate was placed upright in the oven to allow both sides of the plate to be exposed to the water vapor. The furnace was set at 80°C . Because the furnace used in this experiment was not an air shield furnace, the humidity level only reached 75–85%. The water in the tray was refilled every two hours to maintain the moisture level. After the curing process, the plate underwent a drying process at 45°C for 12 hours. Next, the plates were soaked in H_2SO_4 solution with 1.26 sp. gr concentration for four hours in an upright position to allow both sides to be soaked in the solution. Afterwards, the plate was formed using an Autolab potentiostat with a charging cycle of 2A for four hours and then allowed to rest for 30 minutes; this cycle was performed six times.

Preparation of the battery cell was performed using a commercially available positive plate, cut into a rectangular shape of $0.75\text{cm} \times 1\text{ cm}$ in size for each specimen. The positive plate specimen combined with the negative plate of the same size was packed in a small container to hold both plates together with an absorptive glass mat separator in between the plates. All the packed cells were filled with 1.26 sp. gr. H_2SO_4 .

2.2. PSOC Cycling Test

The PSOC testing started with discharging the battery until 50% state of charge or 2.01 Volts open-circuit voltage. In this condition, some sulfation occurred. In the first cycle, which is a discharge cycle, the battery was discharged with 600mA of current for 60 seconds and then charged at 600mA for 60 seconds to simulate the PSOC condition in which the battery did not obtain enough charge, resulting in a very low DoD. The test was run until the battery potential after the discharge cycle reached the cut-off potential of 1.7 volts.

2.3. Electrochemical characterization

Electrochemical characterization consisted of performing cyclic voltammetry (CV) and electrochemical impedance spectroscopy (EIS) tests. The CV test was performed using the

galvanostatic method over the range of 0 V to 1.8 V. The scan rate used was 1.5 mV/s. The size of the plate being tested was 0.75 cm². H₂SO₄ solution used in the previous process with a specific density of 1.28 sp. gr was used. The reference electrode used was Ag/AgCl. The EIS test was performed under the following conditions: frequency range of 10 mHz to 10 kHz, potential of -0.56 V vs. the reference electrode of Ag/AgCl, and perturbation of 10mV. The electrolyte used was H₂SO₄, with a specific density of 1.28 sp. gr. The area of the specimen used was 6 cm². The counter electrode used was a Pb positive plate of 6 cm² in area. The reference electrode was Ag/AgCl. The potential was measured at the end of the cycle.

2.4. SEM characterization

A Hitachi FlexSEM 1000 scanning electron microscope (SEM) was used to examine the sample before and after the PSOC cycle test. The objective was to study the morphology of the sulfate particles. The sample was slightly dried before it was examined in the SEM chamber. The images were taken in the secondary electron image at 20 kV accelerating voltages.

3. RESULTS AND DISCUSSION

3.1. Cycle test at PSOC condition

The result of the cycle test at the PSOC condition is displayed in Figure 1. The two graphs show comparisons of the discharge voltage and the number of charging and discharging cycles for the negative plates with graphene additive and without it. Even though the PSOC testing started with discharging the battery until 50% state of charge and the batteries experienced the same amount of charging and discharging current and time, the plate without graphene reached cut-off voltage at 1140 cycles. In contrast, the plate with graphene reached the cut-off voltage at 1282 cycles.

The graphs in Figure 1 also show that the plate with graphene additive had higher discharge voltage and a gentler slope along with the cycles that might be affected by the polarization of the battery. Polarization refers to an effect that reduces the performance of batteries. The graph proves that graphene additive improves the electrochemical reactions at the interface between the electrode and the electrolyte. However, only performing a life cycle comparison does not completely elucidate the role of the additives in the interface reaction. Thus, the CV test, the EIS test, and SEM inspection were performed to provide insight into the role of the additives.

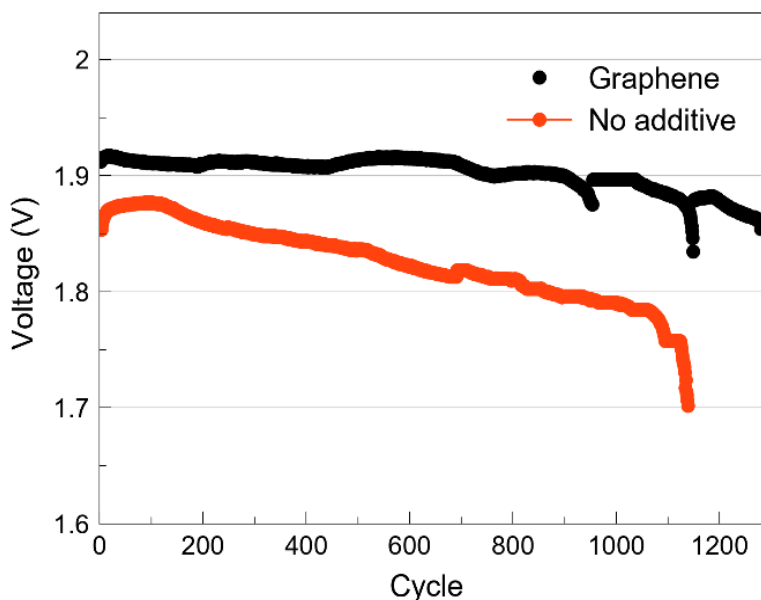


Figure 1. Discharge voltage of the battery with and without graphene during the cycling test. The PSOC test was performed at a constant current of 600 mA for 60 s. The cut of voltage was 1.7 V.

3.2. Cyclic Voltammetry

The cyclic voltammetry test was performed to compare the negative plate's CV curves with and without graphene before and after the PSOC test. The CV curve results before the PSOC test are displayed in Figure 2, and the results after the PSOC test are shown in Figure 3.

Before the PSOC test, the peak current of the plate with graphene additives was 0.3 A/cm^2 , and the peak potential was -0.22 V . The peak current of the plate without graphene was 0.25 A/cm^2 , and the peak potential was -0.3 V . Based on those peak values, the reaction of the plate with graphene additive was found to be slightly more reversible and have a slightly higher faradaic capacity; however, it was revealed that the graphene additive did not improve the capacitance of the plate. A previous study found that the surface area carbon materials [12,22,23] directly influence the capacitance of the LAB cell. The capacitance observed in the present study was low despite the addition of graphene being in the milligram scale; this result is most likely related to the surface area of the graphene used in this study. Figure 3 show that capacitive effect is small enough.

After the PSOC test, the results of the CV curves showed that both negative plates are approximately similar at 0.15 A/cm^2 and that the peak potential was -0.3 V . This result is reasonable because the same PSOC test cut-off voltage was observed on both plates and because both negative plates might still be reversible enough to receive more charging current.

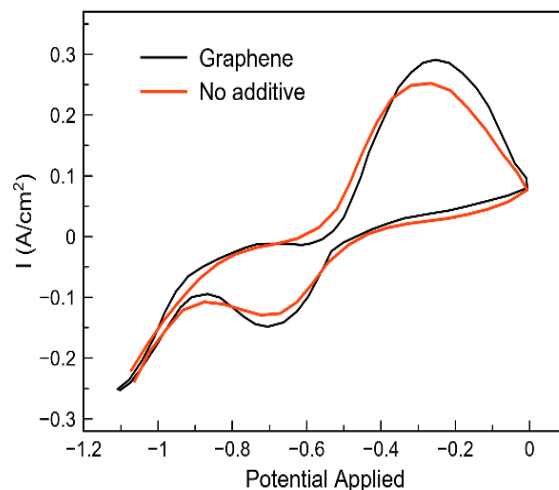


Figure 2. CV graph of the negative plate with and without graphene before the PSOC test. The scan rate during the CV test was 1.5 mV/s.

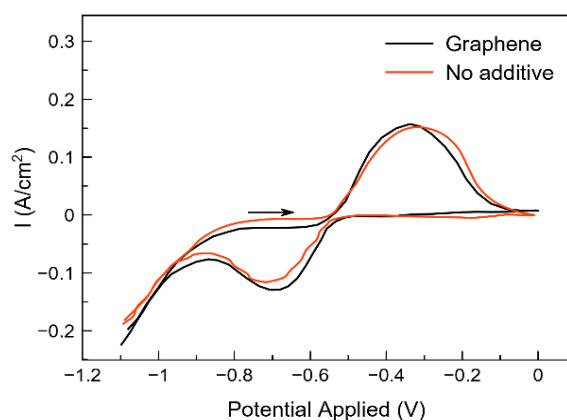


Figure 3. CV graph of the negative plate with and without graphene after the PSOC test. The scan rate during the CV test was 1.5 mV/s.

3.3. EIS Test Results

EIS measurements were performed to develop a Nyquist plot for the negative active plate with and without graphene before the PSOC and after the PSOC test. Figure 4 shows the Nyquist plot before the PSOC test, and Figure 5 shows the Nyquist plot after the PSOC test. Note that the figures are not over the same ranges. The first thing to notice from both figures is that the beginning of the Nyquist plot for the plate with graphene is located more to the left; this observation highlights the resistance of the surface of the plate with graphene and also shows that the solution is more conductive than the plate without graphene. Moreover, the peak of the plot of the plate with graphene is lower than that without the graphene, revealing that the internal conductivity of the plate with graphene is higher. The conductivity of a carbon material, such as graphene, depends on the type of the structural properties; graphene, which has high conductivity, is known to strongly contributes to the conductivity

of the NAM [12,18,24]. Based on the data, it can be concluded that the graphene additive reduces the internal resistance inside the plate and improves the conductance between the plate and the solution. The improvement in conduction is very significant, even after the PSOC test.

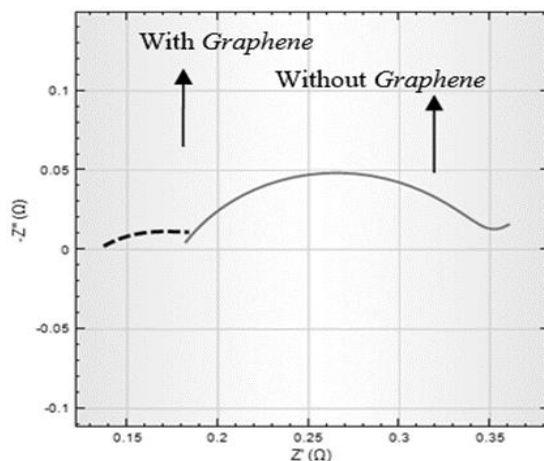


Figure 4. Nyquist plot for the negative plate with and without graphene before the PSOC. The EIS test was performed under the following conditions: frequency range of 10 mHz to 10 kHz, potential of -0.56 V vs. the reference electrode of Ag/AgCl, and perturbation of 10mV.

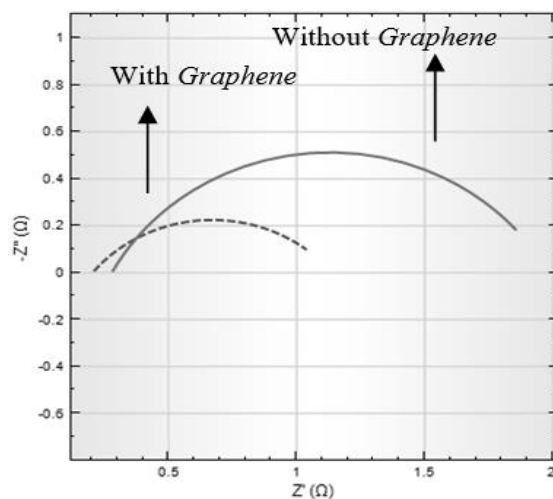


Figure 5. Nyquist plot for the negative plate with and without graphene after the PSOC test. The EIS test was performed under the following conditions: frequency range of 10 mHz to 10 kHz, potential of -0.56 V vs. the reference electrode of Ag/AgCl, and perturbation of 10mV.

The higher conductivity of the plates caused by graphene additive as conductive materials is so significant that it may restrain the additional resistance from the irreversible $PbSO_4$ crystal formation. This finding explains why the plate's discharge voltage with graphene additive has a slightly higher value than the plate without the additive at the PSOC test result before. The gentler slope of the plate

with graphene additive also shows that charge acceptance is improved by improving the conductance of the NAM.

3.4. Sulfate particles

Figure 6 and Figure 7 display SEM images at 2500 \times magnification of the formed PbSO_4 crystals in the negative plate with/without graphene before and after the PSOC test, respectively. Figure 6a shows the image of formed PbSO_4 at the NAM without the graphene additive. Note that, before the PSOC test, the condition of the plate is at 50% DoD, i.e., the PbSO_4 was already formed. The image of the PbSO_4 crystals that are formed in the negative active material (NAM) without the additive appear larger and smoother compared to the PbSO_4 crystals shown in Figure 6b, which shows similar conditions as those of the NAM with the graphene additive. Despite the images being not very clear, it still noticeable that the PbSO_4 crystals have different sizes and a different number of crystal nuclei.

A more noticeable size difference of the PbSO_4 crystals is displayed in the SEM images after the PSOC test presented in Figure 7, which shows the negative plate without and with the addition of graphene sequentially. After the PSOC test, the plate with graphene shows a small particle size of PbSO_4 crystals, whereas the PbSO_4 crystals at the plate without graphene appear to be quite large and smooth. These images clearly highlight that better conduction of the NAM with graphene additive affects the number of nucleation sites of the PbSO_4 crystals and restrain their growth. Moreover, the particle size positively affects the reversibility and charging cycle ability of the battery. Because larger PbSO_4 crystals are more irreversible, the smaller in size they are, the easier they will be to transform back into free Pb, thereby improving the life cycle of the NAM.

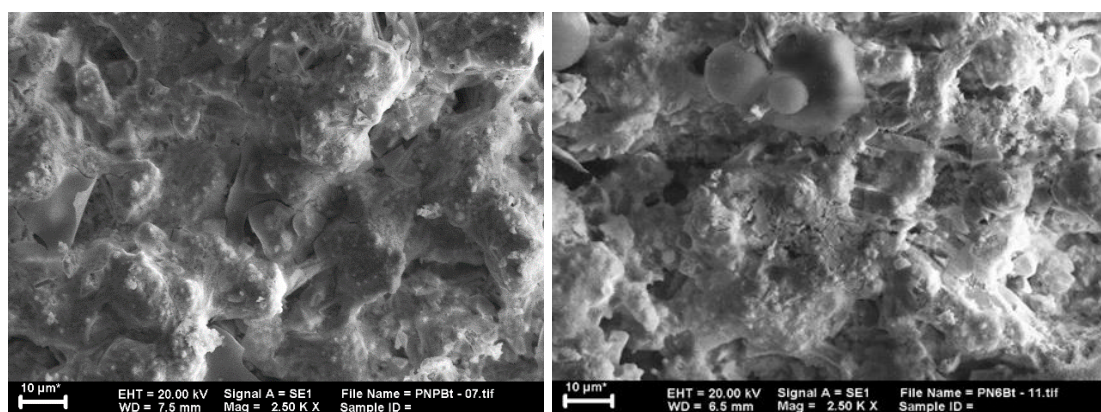


Figure 6. SEM image at 2500 \times magnification of the negative plate without (a) and with graphene (b) before the PSOC test. The SEM image was taken using a 20 kV electron beam and the SEM operating in secondary electron (SE) mode.

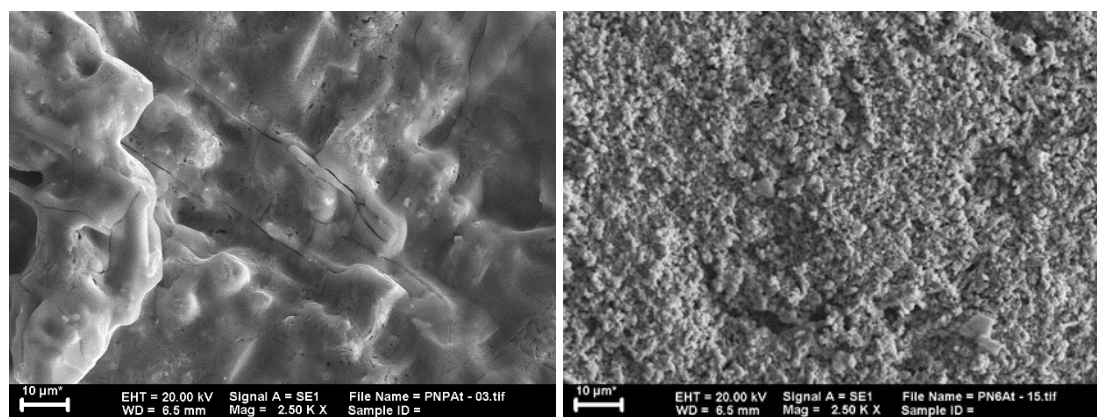


Figure 7. SEM image at 2500× magnification of the negative plate with and without graphene after the PSOC test. The SEM image was taken using a 20 kV electron beam and the SEM operating in secondary electron (SE) mode.

4. CONCLUSION

The experimental results showed that the addition of 0.2 wt.% graphene in a negative active material (NAM) increased the internal and external conductivities of the negative plate. The use of a graphene additive was found to increase the life cycle of the battery despite the plate being at a 50% state of charge before starting the cycle life test, with the charging cycle being identical to the discharging cycle. This condition typically results in reduced lead-acid battery life. The use of graphene as an additive to a NAM was found result in an increase in conductivity. The EIS test showed that the internal and external conductances of the NAM, with a graphene additive before and after the PSOC test were almost twice as high as those without the additive. In the PSOC test, the graphene additive was found to increase the discharge voltage and result in a gentler voltage drop and a longer cycle life. This result proved that graphene is a better conductor compared to other carbon additives.

The PSOC test with a large DoD and small amount of charging resulted in different SEM images of the NAM with the graphene additive compared to those without the additive. The SEM images of the NAM with the graphene additive reveal very small PbSO_4 crystals, whereas the images of NAM without the graphene additive showed large and combined crystals of PbSO_4 . Apparently, graphene's superior conductance increases the NAM conductivity, resulting in the additional capacity to creates more PbSO_4 nuclei of smaller crystals that are less irreversible.

However, the effect of the use of a graphene additive is not clear from the CV test results. The negative plate with graphene addition only has slightly more capacity than that without graphene addition. The capacity improvement is faradaic via the improved conductance of the NAM rather than from a higher capacitance of the NAM. As a result, graphene additives only very slightly improve the capacitance of the negative plate, possibly via the morphology of the graphene used in this study.

ACKNOWLEDGMENTS

The present research was funded by RISTEK Penelitian Disertasi Doktor 2021

References

1. P.P. Lopes, V.R. Stamenkovic, *Science*, 369 (2020) 923–924.
2. P. Ruetschi, *J. Power Sources*, 2 (1977) 3–120.
3. P.T. Moseley, D.A.J. Rand, B. Monahov, *J. Power Sources*, 219 (2012) 75–79.
4. J. Lach, K. Wróbel, J. Wróbel, P. Podsadni, A. Czerwiński, *J. Solid State Electrochem.*, 23 (2019) 693–705.
5. J. Xiang, P. Ding, H. Zhang, X. Wu, J. Chen, Y. Yang, *J. Power Sources*, 241 (2013) 150–158.
6. L.T. Lam, N.P. Haigh, C.G. Phyland, T.D. Huynh, *J. Power Sources*, 144 (2005) 552–559.
7. K.R. Bullock, *J. Power Sources*, 195 (2010) 4513–4519.
8. K. Nakamura, M. Shiomi, K. Takahashi, M. Tsubota, *J. Power Sources*, 59 (1996) 153–157.
9. M. Calábek, K. Micka, P. Křivák, P. Bača, *J. Power Sources*, 158 (2006) 864–867.
10. M. Shiomi, T. Funato, K. Nakamura, K. Takahashi, M. Tsubota, *J. Power Sources*, 64 (1997) 147–152.
11. D. Pavlov, P. Nikolov, T. Rogachev, *J. Power Sources*, 195 (2010) 4435–4443.
12. P.T. Moseley, D.A.J. Rand, A. Davidson, B. Monahov, *J. Energy Storage*, 19 (2018) 272–290.
13. D. Pavlov, P. Nikolov, *J. Power Sources*, 242 (2013) 380–399.
14. D. Pavlov, T. Rogachev, P. Nikolov, G. Petkova, *J. Power Sources*, 191 (2009) 58–75.
15. D. Pavlov, P. Nikolov, T. Rogachev, *J. Power Sources*, 196 (2011) 5155–5167.
16. X. Zou, Z. Kang, D. Shu, Y. Liao, Y. Gong, C. He, J. Hao, Y. Zhong, *Electrochimica Acta*, 151 (2015) 89–98.
17. K.K. Yeung, X. Zhang, S.C. Kwok, F. Ciucci, M.M. Yuen, *RSC Adv.*, 5 (2015) 71314–71321.
18. Q. Long, G. Ma, Q. Xu, C. Ma, J. Nan, A. Li, H. Chen, *J. Power Sources*, 343 (2017) 188–196.
19. A. S, M.K. S, K.U.V. Kiran, S. Mayavan, *J. Energy Storage*, 32 (2020) 101763.
20. L. Dong, C. Chen, J. Wang, H. Li, H. Zheng, W. Yan, J.C.-Y. Jung, J. Zhang, *RSC Adv.*, 11 (2021) 15273–15283.
21. L. Noerochim, J.-Z. Wang, D. Wexler, Z. Chao, H.-K. Liu, *J. Power Sources*, 228 (2013) 198–205.
22. V. Mahajan, R.S. Bharj, *Bull. Mater. Sci.*, 44 (2021) 52.
23. J. Settelein, J. Oehm, B. Bozkaya, H. Leicht, M. Wiener, G. Reichenauer, G. SEXTL, *J. Energy Storage*, 15 (2018) 196–204.
24. V. Mahajan, R.S. Bharj, J. Bharj, *Bull. Mater. Sci.*, 42 (2019) 21.